

Coupled channels analysis of proton scattering from ^{26}Mg

F. Sciuccati, S. Micheletti, and M. Pignanelli

*Dipartimento di Fisica dell'Universita' di Milano, Milano, Italy
and Istituto Nazionale di Fisica Nucleare, Sezione di Milano, Milano, Italy*

R. De Leo

*Dipartimento di Fisica dell'Universita' di Bari, Bari, Italy
and Istituto Nazionale di Fisica Nucleare, Sezione di Bari, Bari, Italy*

(Received 8 August 1984)

Differential cross sections for proton elastic and inelastic scattering by ^{26}Mg have been measured at several proton energies between 15 and 38 MeV. Coupled channels calculations, based on multipole moments predicted by collective and shell-model calculations, have been performed for the g.s., 2_1^+ , 4_1^+ , 2_2^+ , 3_1^+ , 4_2^+ , 4_3^+ , and 3_1^- states. Satisfactory results are obtained at all seven energies for the natural parity levels and also for the 3_1^+ state when a direct $0_1^+ \rightarrow 3_1^+$, $\Delta S = 1$ magnetic coupling is included.

I. INTRODUCTION

Most nuclei in the s - d shell are known to display a rotational band structure characteristic of a deformed nucleus. The inelastic scattering differential cross sections depend therefore on the amplitude and phase of both one-step and multistep excitations, so that coupled-channels (CC) calculations must be performed.

The ^{26}Mg nucleus can be considered soft against gamma deformation because of the low value (1.62) of the ratio $E(2_2^+)/E(2_1^+)$. The $K^\pi = 2^+$ band can therefore also be referred to as a γ -vibrational band in the framework of the rotovibrator model. This model produces for the ground state (g.s.) and γ bands, predictions very similar to those of the asymmetric rotator model. Problems in these CC calculations for ^{26}Mg arise from the difficulty¹⁻³ in classifying its levels in definite rotational bands.

In some cases these problems cause rather large errors even in the predictions of absolute values of the cross sections of excited states. In particular, rotational-model coupled-channels calculations, including only first-order nonspherical quadrupole effects, heavily underestimate the cross section of the 3_1^+ (3.94 MeV) level. This level has been studied recently in proton inelastic scattering at three energies. Data taken at 23.95 MeV (Ref. 4) and 800 MeV (Ref. 5) have been analyzed in a collective approach as belonging, together with the 4_2^+ , to the $K^\pi = 2^+$ band. A direct coupling of $0_1^+ \rightarrow 4_2^+$ (Refs. 5 and 6) or allowing the coupling strengths to differ from the values given by the rigid-rotator model has been found necessary.⁴ Calculations with band mixing⁴ do not improve the results. The 40 MeV data have been analyzed in a shell-model approach⁷ using matrix elements evaluated from the wave functions of Chung and Wildenthal.⁸ Also in this case the 3_1^+ cross section was undervalued.

The aim of the present work is to test the validity of these approaches on data taken at several energies in a large angular range. Cross sections to low-lying levels of ^{26}Mg (including the 3_1^+) have been measured at seven pro-

ton energies between 15 and 39 MeV for the angular range 10° – 170° . The low-energy data are useful in verifying the presence of compound nuclear (CN) contributions. The large angular range permits a significant test of the predicted differential cross sections.

Details on experimental procedure and results are given in Sec. II, and in Sec. III the optical model potentials used in later analyses are obtained. The 3_1^+ data are analyzed in Sec. IV in the framework of the asymmetric-rotor model, and in Sec. V a direct magnetic spin-flip $0_1^+ \rightarrow 3_1^+$ coupling, evaluated microscopically, is coherently included. The 3_1^- (6.88 MeV) data are analyzed in Sec. VI in the framework⁹ of the rotovibrator model.

II. EXPERIMENTAL PROCEDURE AND RESULTS

The experiment was performed using the energy analyzed beam of the Milan sector-focused cyclotron. Cross sections have been measured at 15.0, 17.8, 20.55, 23.4, 27.0, and 38.55 MeV. A solid target isotopically enriched to 97% with an areal density of 1.0 mg/cm² was used. Scattered protons were detected by means of three 3000 μm surface-barrier silicon detectors for $E_p < 23$ MeV, and telescopes of 2000 and 5000 μm detectors for higher energies. The angular distributions were measured in steps of 5° from 10° to 170° laboratory angles. The overall energy resolution, which includes incident beam spread, kinematic broadening, target thickness, and counter resolution varied from 80 to 120 keV. Unfortunately this resolution was not sufficient to resolve the levels of the triplets 4_1^+ , 2_3^+ , and 3_2^+ at 4.3 MeV and 2_4^+ , 4_2^+ , and 0_3^+ at 4.9 MeV. A typical energy spectrum is shown in Fig. 1. The differential cross sections for the g.s., 2_1^+ (1.81 MeV), 2_2^+ (2.938 MeV), 3_1^+ (3.94 MeV), 4_3^+ (5.474 MeV), and 3_1^- (6.88 MeV) levels are shown, respectively, in Figs. 2, 3, 5–7, and 10. The uncertainty in absolute cross section values is estimated to be about 5%. Statistical errors, where significant, are shown as error bars in the figures.

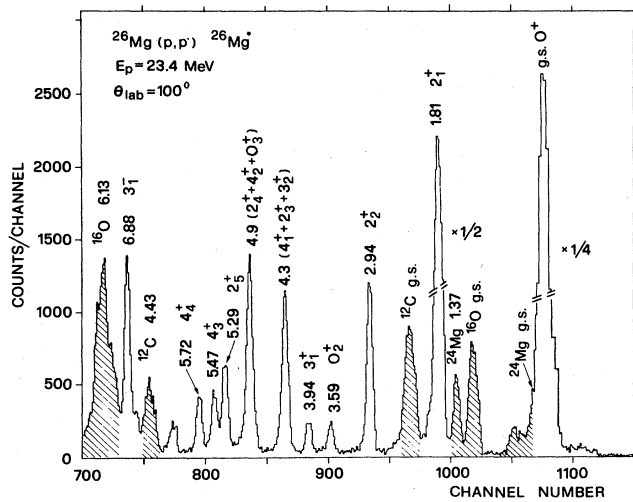


FIG. 1. A typical $^{26}\text{Mg}(p,p')$ spectrum taken at $E_p=23.39$ MeV, $\theta_{\text{lab}}=100^\circ$.

TABLE I. Optical model parameters. The potential listed is of the form:

$$U(r) = -V_0 f(x_0) - i \left[W_v f(x_w) - 4W_d \frac{d}{dx_w} f(x_w) \right] + V_{\text{so}} \left[\frac{\hbar}{m_p c} \right]^2 \left[\frac{1}{r} \right] \left[\frac{d}{dr} \right] f(x_{\text{so}}),$$

where $f(x_i)$ is a Woods-Saxon form factor with $x_i = (r - R_i A^{1/3})/a_i$ and where $V(r, R_C)$ is the Coulomb potential of a uniformly charged sphere of radius $R_C = 1.2A^{1/3}$. (Potential depths are in MeV and geometrical parameters in fm).

V_0	$55.62 - 0.319E_p$
r_0	1.15
a_0	0.65
W_v	$0.149E_p - 2.24$ for $E_p < 23.4$ MeV $0.245E_p - 4.48$ for $E_p \geq 23.4$ MeV
W_d	$6.88 - 0.12E_p$
r_w	1.32
a_w	0.6
V_{so}	5.6
r_{so}	1.01
a_{so}	0.6

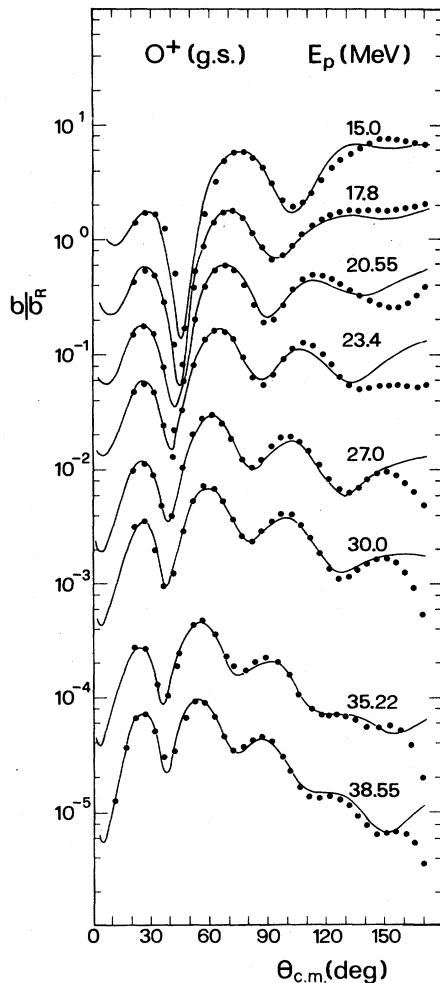


FIG. 2. Differential cross sections (points) for proton elastic scattering on ^{26}Mg . The full curves are the result of g.s., 2_1^+ coupled-channels calculations.

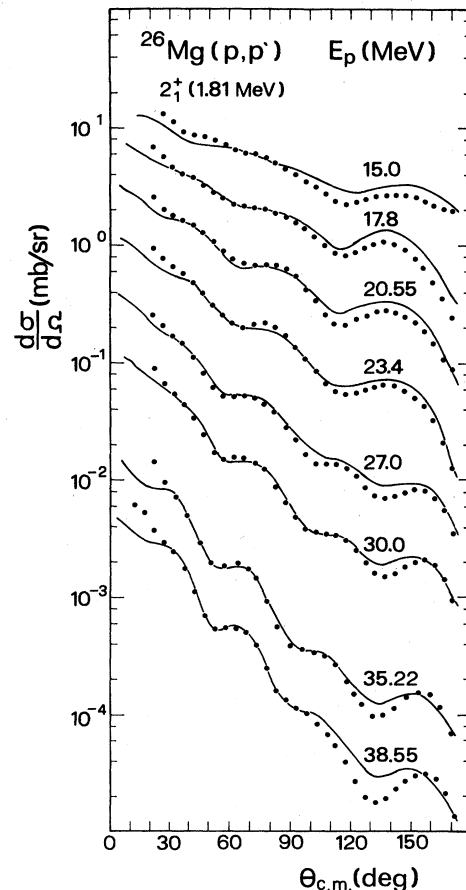


FIG. 3. Differential cross sections for proton inelastic scattering from the 2_1^+ state. The full curves are the result of g.s., 2_1^+ coupled-channels calculations.

III. THE GROUND STATE BAND

The optical model potential used in the subsequent analyses was obtained in a coupled-channels, symmetric rotational model search procedure on the g.s. and 2_1^+ differential cross sections at all the energies. This was limited to data up to $\theta_{lab}=120^\circ$ to avoid the inclusion of effects caused by the backward maximum due¹⁰ to couplings with highly excited inelastic or deuteron channels. After a preliminary search, the spin orbit and the geometrical parameters of the real and imaginary central terms were fixed at energy-independent values. The potential depths were required to show a smooth energy dependence; the results obtained in the final search are given in Table I. The fits obtained are shown in Figs. 2 and 3 and, as expected, do not reproduce the backward peak in the elastic data.

IV. ASYMMETRIC ROTOR MODEL CALCULATIONS

Nuclei in the $2s-1d$ shell are considered to be permanently deformed in their ground state. The collective nature of ^{26}Mg has not been studied as extensively as that of other nuclei in this region. Although the existence, and strong excitation in inelastic scattering, of two 2^+ low-excitation states indicates¹¹ violation of axial symmetry, the assignment of its many low-lying states to the specific bands expected on the basis of the asymmetric rotor or rotovibrator models is not yet firmly established. Particularly interesting is the presence of two unnatural-parity 3^+ states. The excitation mechanism of these states in inelastic scattering has been the object of extensive interest.^{4,5,6,12} Two-step processes involving the 2^+ states cited already and the 4^+ state belonging to the same band contribute significantly to their excitation. The excitation of the 2^+ states can be reproduced satisfactorily by the triaxial rotor model also when the coupling potential is evaluated neglecting higher-order terms in the nuclear radius Legendre expansion:

$$R(\theta', \phi') = R_0 \left[1 + \sum_{\lambda\mu} \alpha_{\lambda\mu} Y_{\lambda\mu}(\theta', \phi') \right], \quad (1)$$

where the primes indicate the body fixed coordinate system. Truncation of this expansion in the analysis of low-lying states is justified by the decreasing effect of larger multipoles.

The excitation of the γ -band 4^+ states in the $s-d$ shell⁴⁻⁷ and also in some actinide and rare-earth nuclei¹³ can only be explained with a direct excitation from the ground state. This coupling can be taken into account in the triaxial model considering also the $(Y_{4,2} + Y_{4,-2})$ term in the expansion.

We have considered the following terms in the multipole expansion, written following Tamura¹² as

$$R = R_0 \left\{ 1 + \beta_2 \left[\cos\gamma_2 Y_{20} + \frac{\sin\gamma_2}{\sqrt{2}} (Y_{2,2} + Y_{2,-2}) \right] + \beta_4 \left[\cos\gamma_4 Y_{4,0} + \frac{\sin\gamma_4}{\sqrt{2}} [\cos\gamma_5 (Y_{4,2} + Y_{4,-2}) + \sin\gamma_5 (Y_{4,4} + Y_{4,-4})] \right] \right\}. \quad (2)$$

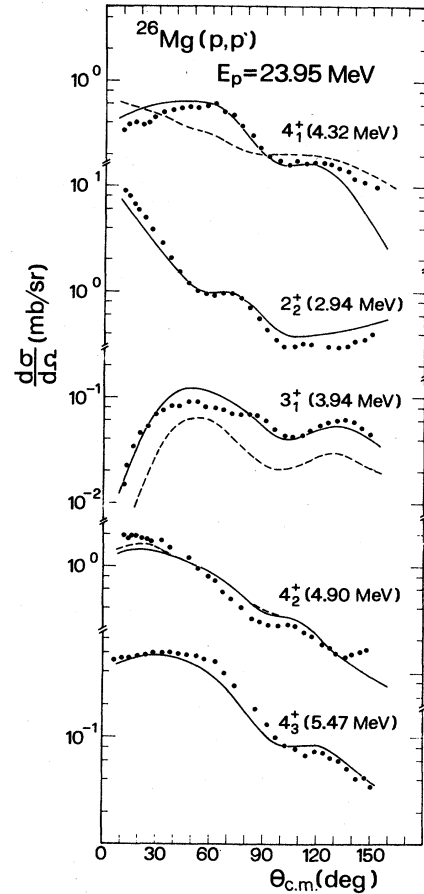


FIG. 4. CC analysis of the data of Ref. 4. The full curves show the results obtained for increased RNME values (see the text).

The terms containing the parameters γ_2 , γ_4 , and γ_5 give rise to direct couplings between the g.s. and the 2^+ and 4^+ states of the $K^\pi=2^+$ band, and the 4^+ head of the $K^\pi=4^+$ band, respectively. The term containing γ_5 adds transitions with $\Delta K=4$ to those with $\Delta K=0$ between the levels within the $K^\pi=2^+$ band. In this case the number of couplings given by the asymmetric rotor model is larger than that of the rotovibrator model in the form used in Refs. 6 and 11.

The difficulty encountered in assigning the low-lying levels, and particularly the lowest 4^+ , to particular rotational bands indicates the presence of band mixing. The latter has been considered in the literature,¹⁴ but not in studies including the 3_1^+ state. This level and the 3_2^+ have been described, respectively, as head of the $K^\pi=3^+$ and as member of the $K^\pi=2^+$ bands in electromagnetic (em)

TABLE II. Coupled-channels analysis deformation parameters.

	β_2	γ_2 (deg)	β_4	γ_4 (deg)	γ_5 (deg)
CC1:	0.39	23.3	-0.22	-109.2	33.7
CC2:	0.37	28.6	0.30	26.9	

studies.¹⁵ Previous asymmetric rotor analyses⁴⁻⁶ of (p,p') experiments assume $\gamma_5=0$ and K to be a good quantum number (no band mixing). Their results seem to favor the assignment of the 3_1^+ state to the $K^\pi=2^+$ band. Two of these analyses refer to the data of Alons *et al.*⁴ at 23.95 MeV, which separate the 3_2^+ and the 4_1^+ levels in the triplet of states at 4.3 MeV.

For this reason we have used the same data to carry out a preliminary coupled-channels analysis to determine the β_i and γ_i parameters. This analysis assumes the $(0_1^+, 2_1^+, 4_1^+)$, $(2_2^+, 3_1^+, 4_2^+)$, and 4_3^+ levels to belong to the $K^\pi=0^+$ (g.s.), 2^+ , and 4^+ bands, respectively. This and all the following CC analyses have been performed using the code ECIS.¹⁶ The fits obtained are shown by the dashed lines in Fig. 4 and the deformation parameters (CC1) are given in Table II.

It should be noted that the shapes of the angular distributions of the 4_2^+ and 4_3^+ states differ significantly. These, and also the absolute cross section values, are well reproduced by our analysis which therefore supports the preceding assignments. The inadequacy of the rigid rotor assumption is especially evident in the poor reproduction of the 4_1^+ shape. This has been improved upon by Alons

*et al.*⁴ by decreasing the reduced nuclear matrix elements (RNME) of the $L=4, 0_1^+ \rightarrow 4_1^+$ and $L=2, 4, 2_1^+ \rightarrow 4_1^+$ coupling terms with respect to their asymmetric rotor values. We have found a much improved fit, shown in Fig. 4 by the full line, reducing only the $L=2$ RNME's for the second transition from -1.6 to 0.875 . This reduction (antistretching) reflects the experimental value for the ratio

$$\frac{B(E2, 4_1^+ \rightarrow 2_1^+)}{B(E2, 2_1^+ \rightarrow 0_1^+)}, \quad (3)$$

which is significantly lower than that given by the rotational model without band mixing. The low value of this ratio substantiates also the hypothesis that the g.s. band 4^+ strength in ^{26}Mg is fragmented over several levels.

The calculated angular distribution for the 3_1^+ state is well reproduced but the absolute cross section is seriously undervalued. This failure is not directly connected with the choice of the 4_2^+ level as a third member of the $K^\pi=2^+$ band since the 4_2^+ and 4_3^+ cross section absolute values are similar within a factor of 2.

A correct absolute value is only obtained when the

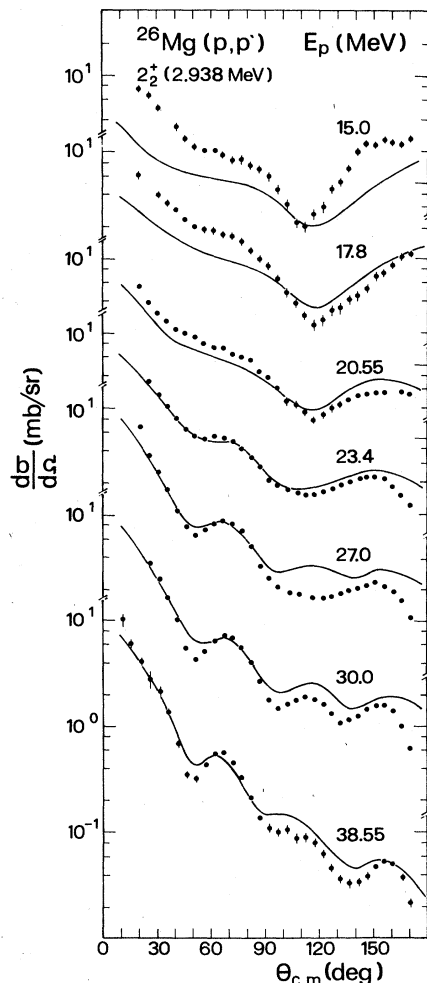


FIG. 5. Differential cross sections for scattering from the 2_2^+ state. The full curves have the same meaning as in Fig. 4.

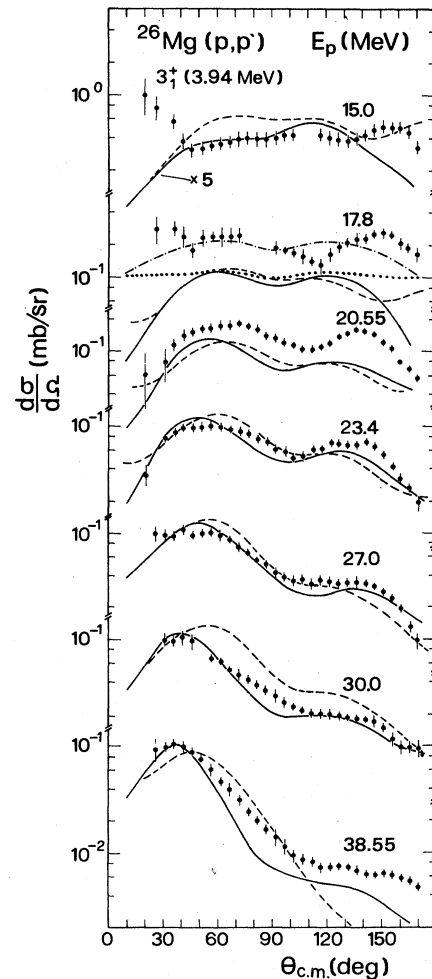


FIG. 6. Differential cross sections for scattering from the 3_1^+ state. The full curves have the same meaning as in Fig. 4.

RNME's of the couplings within the $K^\pi=2^+$ band are increased. This increase does not deteriorate the quality of the fits to the 2^+ and 4^+ in the same band and corresponds to the hypothesis that the deformations (and therefore the momenta of inertia) of the $K^\pi=2^+$ differ from those of the g.s. band. This hypothesis is part of the rotovibrator model and results in the introduction⁶ of the β_2^γ parameter.

The full curve in Fig. 4 is obtained with $L=2$ RNME's increased by about 60%. This corresponds to a ratio between the momenta $J_{g.s.}/J_{K^\pi=2^+}=0.39$ which is about 30% smaller than the value 0.55 obtained¹¹ from the ratio of the energies of the first two levels of the two bands.

These modifications of the $L=2$ RNME's (i.e., reduction of that corresponding to the $2_1^+ \rightarrow 4_1^+$ transition and increase of those within the $K^\pi=2^+$ band) are not mutually influenced, in the sense that the first affects only the 4_1^+ and the second affects only the 3_1^+ cross section.

If the couplings with the 4_3^+ level are omitted ($\gamma_5=0$), only the cross section of the 3_1^+ is affected. Its shape remains the same but its absolute value is lowered. The latter can be again brought in agreement with the experi-

ment by increasing the RNME's within the $K^\pi=2^+$ band by a factor of 2 with respect to their asymmetric-rotor values. In this case the best-fit value of γ_4 decreases from -109 , reported in Table III, to -70 .

A first coupled-channels calculation (CC1) has been performed for all the incident proton energies with the parameters which produce the full curves of Fig. 4. The results are shown in Figs. 5–7 (full curves) for the 2_2^+ , 3_1^+ , and 4_3^+ levels, respectively. The energy behavior of the cross sections is well reproduced for all the energies except the two lowest ones. When compound nucleus contributions, evaluated as in Ref. 6, are added, good results are obtained also at low energies. This is shown in Fig. 6 for the 3_1^+ data at 17.8 MeV. The dotted curve represents the compound nucleus contribution alone and the dotted-dashed curve represents the total cross section obtained as the incoherent sum of both contributions.

A second (CC2) asymmetric-rotor coupled-channels calculation with $\gamma_5=0$ and the 4_3^+ level, instead of the 4_2^+ , as a member of the $K^\pi=2^+$ band, has been performed in order to test the sensitivity of 3_1^+ cross section calculations to model assumptions. This band assignment has been

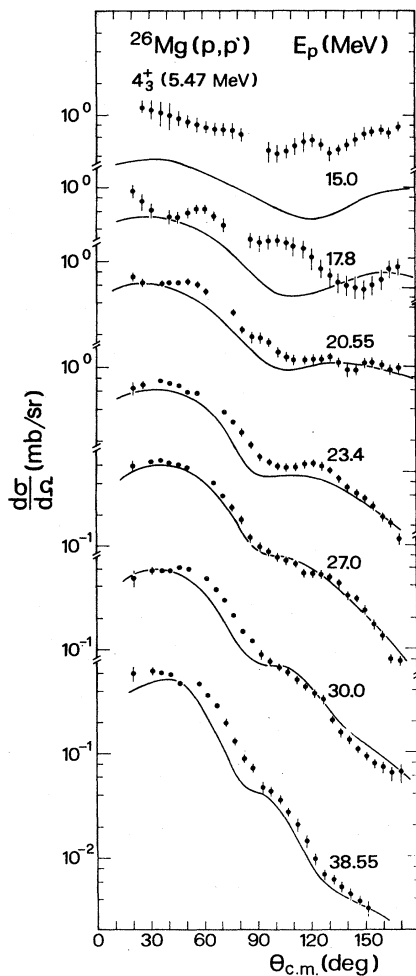


FIG. 7. Differential cross sections for scattering from the 4_3^+ state. The full curves have the same meaning as in Fig. 4.

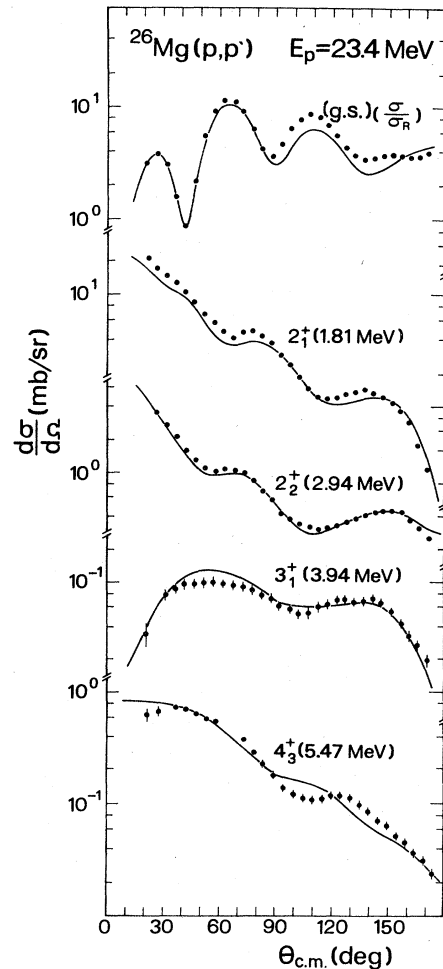


FIG. 8. Experimental and calculated cross sections at 23.4 MeV. The full curves are the result of CC calculations in the CC2 scheme (see the text).

TABLE III. Transition strengths.

$J_i \rightarrow J_f$	λ	$M_{p,p'}$ values from CC1 analysis	$M_{p,p'}$ values from CC2 analysis	$M_{p,p'}$ values from CC3 analysis	Electromagnetic M_{em} values	Shell-model $M_{p,p'}$ values from Ref. 1	Shell-model E_{em} values from Ref. 1
$0_1^+ \rightarrow 2_1^+$	2	-18.36	-17.82	19.45	17.32 ± 0.7^a	14.36	16.9
$0_1^+ \rightarrow 2_2^+$	2	-6.71	-7.44	8.0	3.08 ± 0.4^a	8.46	4.04
$0_1^+ \rightarrow 3_1^+$	2			$3.1 \pm 1.$	8.73		
$0_1^+ \rightarrow 4_1^+$	4	101.0	153.7	$110.3 \pm 4.$	67.75^a	82.3	36.25
$2_1^+ \rightarrow 2_2^+$	2	-8.06	-8.9	-11.83	$11.83^{a,c}$	-14.3	11.61
	4	183.7	154	73.53		76.9	
$2_1^+ \rightarrow 3_1^+$	2	10.5	11.76	0.28 ± 0.07	$\leq 0.173^a, 0.49^b$	0.3	1.27
	4	116.6	230.3	-140.0		-140.	
$2_1^+ \rightarrow 4_1^+$	2	-7.7	-7.48	7.42 ± 1.5		7.79	
	4	161.1	91	4.9	-8.04 ^a	5.10	
$2_2^+ \rightarrow 3_1^+$	2	-46.5	-59.7	-0.48 ± 0.55	$\leq 4.47^a$	-0.48	0.147
	4	29.0	185	-2.65		-2.65	
$2_2^+ \rightarrow 4_1^+$	2	-10.5	-39.1	-9.35	$\leq 9.49^a$		7.76
	4	124.3	328	61.28		56.0	
$3_1^+ \rightarrow 4_1^+$	2	-7.9	-58.8	-23.2	21.17 ± 5.7^a	-23.2	24.14
	4	-223.9	-205	-30.64		-30.4	
$0_1^+ \rightarrow 3_1^-$	2			28.4	27.57 ± 11.8^a		

^aP. M. Endt, At. Data Nucl. Data Tables 23, 3 (1979).^bP. Wagner *et al.*, Phys. Rev. C 11, 1622 (1974).^cP. M. Endt and C. van der Leun, Nucl. Phys. A310, 1 (1978).

suggested¹⁷ on the basis of γ -decay transition rates. The best fit deformation parameters used are given in Table II. Also in this case the $L=2$ RNME's within the $K^\pi=2^+$ band must be increased by a factor of 2 to reproduce the absolute value of the 3_1^+ cross sections. The results obtained for our data at 23.4 MeV are shown in Fig. 8. They are of the same quality as those given by CC1. The same is true for the other energies.

V. COMPARISON OF TRANSITION STRENGTHS

The (p,p') electric multipole moments of the matter density can be obtained, using Satchler's theorem,¹⁸ from those of the optical potential which are defined as:¹⁹

$$M_{p,p'}(E\lambda, J_i \rightarrow J_f) = Ze \text{ RNME} \frac{\int V_{\text{trans}} r^{2+\lambda} dr}{\int V_{\text{opt}} r^2 dr} (e \text{ fm} \lambda). \quad (4)$$

Both real and imaginary central terms are considered in the transition and optical potentials. The values obtained in the preceding CC analyses are reported in the third and fourth columns of Table III. The sign in front of the $M_{p,p'}(E\lambda)$ values is that which must be given to the RNME's in the code ECIS. The sixth column gives the corresponding em values obtained in electromagnetic measurements. Multipoles from electromagnetic data depend only on electric charge distributions and therefore only on proton excitations, while those obtained from proton inelastic scattering are determined by both proton M_p and neutron M_n matrix elements. Their explicit dependence can be written⁴ as

$$M_{p,p'} = \frac{1}{V_{pp} + V_{pn}} (V_{pp} M_p + V_{pn} M_n), \quad (5)$$

where V_{pp} and V_{pn} denote the interaction strength between the incident proton and a target proton or neutron, respectively. Consequently the $M_{p,p'}/M_{\text{em}}$ ratios should be equal to one only for $M_p = M_n$, and lower or higher than one for predominantly proton or neutron transitions.

The values calculated for $M_{pp'}$ and M_{em} in Ref. 7 from the shell model eigenfunctions of Chung-Wildenthal are given in the seventh and eighth columns, respectively.

Well-determined values for M_p and M_n in ^{26}Mg are found in the literature relative to the transitions $0_1^+ \rightarrow 2_1^+$ and $0_1^+ \rightarrow 2_2^+$. They have been obtained combining information from several sets of experiments: proton scattering and em measurements,⁴ proton and neutron scattering,²⁰ π^+ and π^- scattering,²¹ and em measurements relative to ^{26}Mg and its mirror nucleus ^{26}Si .²² Our $M_{pp'}$ values for the two preceding transitions are in good agreement with those given in the literature, while those for the $L=2$, $2_1^+ \rightarrow 3_1^+$ and $2_2^+ \rightarrow 3_1^+$ transitions are very large and would require matrix elements much larger than those given by shell-model calculations.⁴ No electromagnetic values are available for comparison with the $L=4$ components.

These large values and the modifications of those of the RNME's for the transitions within the γ band with respect to those given by the rotator model may compensate for the absence of a direct magnetic excitation of the

3_1^+ state in this model.

The effect produced by the incoherent addition of this coupling has been tested by Zwiaglinski *et al.*⁷ at 40 MeV and found to be important. They attribute the fact that their calculation still underestimates the 3_1^+ cross section to the absence of the interference terms. The analysis⁵ of the 800 MeV data does not include this coupling and also predicts a 3_1^+ cross section lower than the data.

VI. COUPLED-CHANNELS ANALYSIS WITH THE INCLUSION OF THE DIRECT MAGNETIC EXCITATION OF THE 3_1^+ STATE

The preceding comparison of multipole moments suggests a complete coupled-channels calculation, including the direct excitation of the 3_1^+ state via a $\Delta S=1$ magnetic coupling with the g.s. This is possible only abandoning the collective rotor models.

For this direct excitation we have used a microscopic form factor obtained from the DWBA72 code.²³ In this code form factors are factorized into two parts each multiplying an elementary matrix spanning the spin space of the interacting particles. For "unnatural parity" these are denoted as C and D form factors. They have been combined linearly²⁴ to obtain the $L=2$ and $L=4$ form factors required by the ECIS code. The microscopic calculation includes both central and noncentral components of the $M3Y$ (Ref. 25) two-body interaction. It utilizes the "single-channel" optical potentials of Table I and shell-model amplitudes obtained from the wave functions of Chung and Wildenthal.

For all the other "natural parity" transitions, standard form factors given by first derivatives of the optical potential V_{opt} have been used. The suffix "opt" refers to the real, imaginary, and spin-orbit parts of V_{opt} . Only couplings for which M_{em} and the shell model $M_{p,p'}$ exist, and have appreciable values, have been considered.

CC calculations have been first performed at 38.55 MeV to evaluate the effect of the different contributions and of the inclusion of an imaginary part in the direct $0_1^+ \rightarrow 3_1^+$ coupling. The RNME's for the different transitions have been taken at their shell-model values given in Table III, and that relative to the $0_1^+ \rightarrow 3_1^+$ coupling has been adjusted in a best-fit procedure. The resulting $M_{p,p'}$ value is lower than the electromagnetic one and could indicate a predominance of proton contributions in the latter transition. Subsequently, also the other (p,p') matrix elements have been adjusted; their best-fit values (CC3 in Table III) are generally not very different from those given by shell-model calculations. In particular, increasing, within reasonable limits, the values of those between levels in the $K^\pi=2^+$ band changes the 3_1^+ cross section very little. The fits obtained at 38.55 MeV are shown in Fig. 9.

An imaginary part in the direct coupling has been added in the following way. We have used the DWBA form factor which results from the folding of the $M3Y$ nucleon-nucleon interaction over the transition density and multiplying the result by the density dependence given by Jeukenne *et al.*²⁶ for the real and imaginary parts.

The dashed curve shows the effect on the 3_1^+ level of

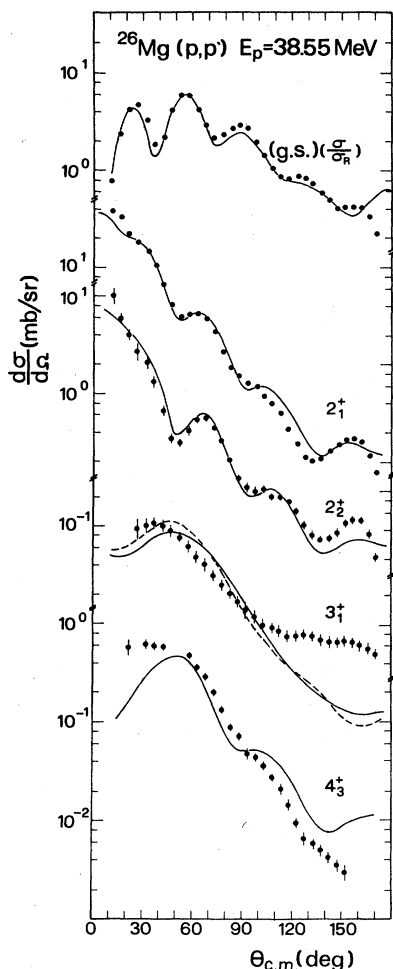


FIG. 9. Experimental and calculated cross sections at 38.55 MeV. The lines are the result of CC calculations, including a direct magnetic term.

the inclusion of the imaginary part. Both terms have been renormalized in order to keep the total multipole moment constant. The fits obtained for the 3_1^+ with the same parameters at the lower energies are shown in Fig. 6 by the dashed lines. Absolute values are well reproduced with the exception of the two lowest energies.

VII. THE 3_1^- STATE

The 6.88 MeV state has been determined to be $J^\pi=3^-$ in (e,e') analyses.²⁷ It can be excited in the rotovibrator model either with a Y_{30} or a $(Y_{33} + Y_{3-3})$ multipole. The first mode corresponds to its assignment to the $K^\pi=0^-$ band, as suggested in Ref. 5; the second corresponds to taking it as head of the $K^\pi=3^-$ band. CC calculations, in which this level is coupled the 0_1^+ and 2_1^+ , have been performed using the code CHUCK.²⁸ The coupling to the 2_1^+ state has been found to give an appreciable contribution. The optical model parameters of Table I have been used and the quadrupole deformation parameter of the octupole rotational band, β_2^{oct} , has been taken equal to that

of the g.s. band. The results from the second assignment are shown in Fig. 10 (full curves). A good overall fit is obtained for all the energies, except the two lowest ones, where compound-nucleus effects are important. An octupole deformation value $\beta_3=0.18$ has been obtained. It corresponds, as shown in Table III, to an electric octupole moment $M(E3)$ in good agreement with the electromagnetic value.²⁶

The results obtained assuming the first mode ($K^\pi=0^-$) are shown for the four higher energies by the dashed lines. These have been normalized to the $K^\pi=3^-$ calculations in the first maximum. The normalization required at the different energies is the same and corresponds to an 18% decrease of the β_3 value. The quality of the fits obtained with this assignment is equivalent to that with $K^\pi=3^-$ at 23.4 and 27 MeV and becomes slightly worse with in-

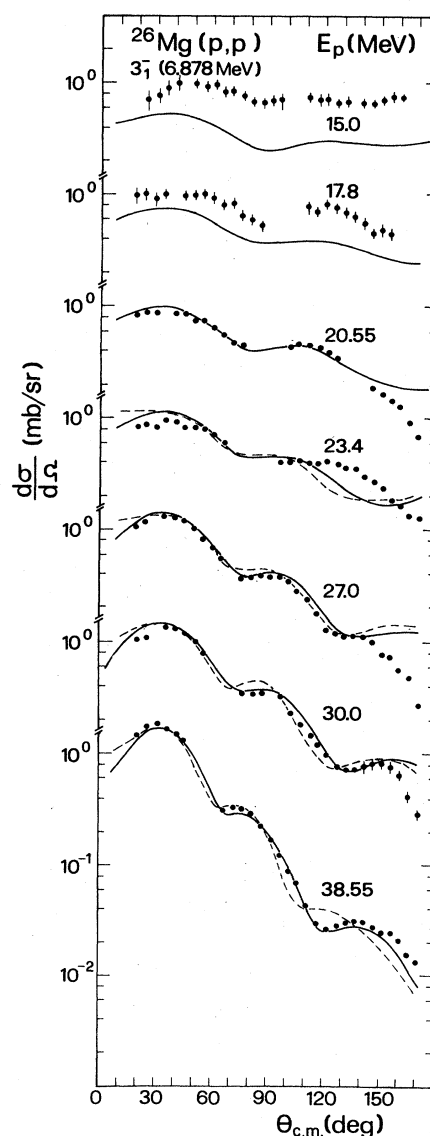


FIG. 10. Differential cross sections for scattering from the 3_1^- state. The full curves are the result of rotovibrator CC calculations assuming $K^\pi=3^-$. The dashed curves at the higher energies assume $K^\pi=0^-$.

creasing energy due to a shift in the position of the maxima at larger angles. Although CC calculations in this energy range are not very sensitive to a choice between the two possible assignments, this worsening of the $K^\pi=0^-$ fits seems to favor a $K^\pi=3^-$ assignment in contrast with that based⁵ on the analysis of the 800 MeV data.

VIII. CONCLUSIONS

CC asymmetric-rotor model calculations, including the $(Y_{4,2} + Y_{4,-2})$ term, have been compared with (p,p') g.s. and γ -band level cross sections at several energies. Because of the ambiguous band assignment, the rotational analysis has been repeated twice, assuming, respectively, the 4_2^+ and the 4_3^+ levels as third members of the $K^\pi=2^+$ band. It has been shown that good quality fits for all the levels considered, excluding the 3_1^+ , can be obtained at all

the energies considered by reducing (antistretching) only the $L=2$ RNME for the $2_1^+ \rightarrow 4_1^+$ transition. Multipole moments of transitions which do not involve the 3_1^+ level are in agreement with em data. The 3_1^+ cross sections result in both cases smaller than the experimental ones, and the values of best fit $L=2$ multipole moments for the $2_1^+ \rightarrow 3_1^+$ and $2_2^+ \rightarrow 3_1^+$ transitions result larger than those from em data. Correct results for the 3_1^+ cross sections at all the energies and multipole moment values in good agreement with those from em data are instead obtained in a full CC calculation, which includes the magnetic term causing the direct $0_1^+ \rightarrow 3_1^+$ coupling. A microscopic form factor has been used for this coupling.

The 3_1^- (6.88 MeV) data have been analyzed in the framework of the rotovibrator model. The results seem to favor its assignment as head of the $K^\pi=3^-$ band.

¹A. Nagel *et al.*, *J. Phys. G* **1**, 234 (1975).

²G. Craig, *Nucl. Phys. A* **225**, 493 (1974).

³N. M. Clarke, *J. Phys. G* **6**, 865 (1980).

⁴R. W. F. Alons *et al.*, *Nucl. Phys. A* **367**, 41 (1981); *Phys. Lett.* **83B**, 34 (1979).

⁵G. S. Blanpied *et al.*, *Phys. Rev. C* **25**, 422 (1982).

⁶R. De Leo *et al.*, *Phys. Rev. C* **23**, 1355 (1981).

⁷B. Zwiaglinski *et al.*, *Phys. Rev. C* **28**, 542 (1983).

⁸W. Chung, Ph.D. thesis, Michigan State University, 1976 (unpublished); B. H. Wildenthal, *Nukleonika* **23**, 459 (1978).

⁹M. N. Harakeh, the code BEL, Kernfysisch Versneller Instituut Report No. 77i, 1981; K. van der Borg *et al.*, *Nucl. Phys. A* **325**, 31 (1979).

¹⁰E. Fabrici *et al.*, *Phys. Rev. C* **21**, 844 (1980).

¹¹A. S. Davidov and G. F. Filippov, *Nucl. Phys.* **8**, 237 (1958).

¹²T. Tamura, *Nucl. Phys.* **73**, 241 (1965).

¹³F. Todd Baker *et al.*, *Phys. Rev. C* **17**, 1559 (1978); R. S. Mackintosh, *Phys. Lett.* **29B**, 629 (1969).

¹⁴N. M. Clarke, *J. Phys. G* **6**, 865 (1980).

¹⁵P. Wagner *et al.*, *Phys. Rev. C* **11**, 1622 (1975); K. Dybdal *et al.*, *Nucl. Phys. A* **359**, 431 (1981).

¹⁶J. Raynal, the code ECIS, private communication.

¹⁷J. L. Durell *et al.*, *J. Phys. A* **5**, 302 (1972).

¹⁸G. R. Satchler, *J. Math. Phys.* **13**, 1118 (1972).

¹⁹D. M. Brink and G. R. Satchler, *Angular Momentum* (Oxford University, Oxford, 1968).

²⁰R. C. Taylor *et al.*, *Nucl. Phys. A* **401**, 237 (1983).

²¹C. A. Wiedner *et al.*, *Phys. Lett.* **97B**, 37 (1980).

²²A. M. Bernstein *et al.*, *Phys. Rev. Lett.* **42**, 425 (1979); *Phys. Lett.* **130B**, 255 (1980).

²³J. Raynal, the code DWBA, private communication.

²⁴J. Raynal, private communication.

²⁵G. Bertsch *et al.*, *Nucl. Phys. A* **284**, 399 (1977).

²⁶J. P. Jeukenne *et al.*, *Phys. Rev. C* **16**, 80 (1977).

²⁷E. W. Lees *et al.*, *J. Phys. A* **7**, 936 (1974).

²⁸P. D. Kunz, the code CHUCK, University of Colorado.